BMC Chemistry

RESEARCH

Open Access

Effect of H_2O_2 and pH on properties of myofibrillar proteins from Yak muscle during thermal gelation process

Sha Qu[1], Dong Sun[2], Ting Hu[1] and Gang Hao[1*]

Abstract

This paper examined the thermal gelation of yak myofibrillar protein (MP) incubated in a Fenton oxidation system at different pH values for 24 h. The effect of protein oxidation on the gel properties at different pH levels was explored by studying the water-holding capacity (WHC), solubility, texture, and other characteristics, while the chemical force, rheological, and microstructural variation in these conditions were analyzed. The results showed that protein oxidation negatively impacted the yak meat MP gel characteristics ($p < 0.05$). Increasing the H_2O_2 interval at different pH levels significantly decreased ($p < 0.05$) the WHC, solubility, and texture of the protein gel, the average reduction was 7.5%, 27.5%, 12.5% respectively. The H_2O_2 concentration and pH level substantially affected ionic and hydrogen bond formation ($p < 0.05$). Oxidation had the most obvious impact on the gel characteristics at pH 5.0. The MP gel displayed a loose, disordered microstructure with the lowest WHC, textural strength, storage modulus (G′), and intermolecular protein force. Oxidation had the least impact on the gel properties at pH 6.0. The MP gel exhibited the highest textural strength, G′, and intermolecular forces, characterized by a compact, orderly microstructure with small, uniformly distributed pores. The gel displayed the best WHC after oxidation at pH 8.0.

Keywords Yak, Myofibrillar protein, pH, Gel, fenton system

Introduction

Gelation, a crucial functional property of myofibrillar protein (MP), affects the quality of meat products. Protein gelation involves the ordered denatured molecule aggregation to form a continuous network [1]. Extensive research on heat-induced gelation during food processing is available since it is responsible for the structure of many foods [2]. Thermal gelation is a complex process involving several steps, such as denaturation, dissociation-association, aggregation, and three-dimensional network formation [3]. Denaturation is a prerequisite for gel formation, causing partial protein unfolding and exposing previously buried hydrophobic groups [4]. Exposed residues in unfolded proteins interact through non-covalent interactions, including hydrogen bonds, electrostatic interactions, and disulfide bonds, leading to aggregation and the formation of complex network structures [5] Aggregation is crucial during heat-induced gelation. Gelation conditions can influence the shapes, sizes, and molecular weights of aggregates, ultimately affecting network structure and gel properties [6].

Intrinsic and extrinsic factors influence protein gelation types and properties [6]. Intrinsic factors are related

*Correspondence:
Gang Hao
indianahg@hotmail.com
[1]College of Pharmacy and Food, Southwest Minzu University, ChengDu 610041, China
[2]College of Food and Biotechnology, Sichuan Vocational and Technical College, Suining 629000, China

to the protein perse, including electrostatic interactions, disulfide bonds, thiol-disulfide interchange, molecular weight, amino acid composition, and hydrophobicity [7]. Extrinsic factors include the environmental conditions surrounding the proteins, such as temperature, pH, ionic strength, protein concentration, salt type, and pressure. pH is a primary factor affecting the gel structure and properties, influencing the counterbalancing attraction and repulsion forces between the protein molecules by changing the MP molecule charge. The force between protein molecules can also be modified by adjusting the protein isoelectric point (pI) to change the MP gel [5]. A net protein pI charge equal to zero decreases the intermolecular electrostatic repulsion force. Therefore, the aggregation speed of the denatured polypeptide chains accelerates, reducing orderly aggregate formation, which decreases the gel transparency and increases the coarseness. The protein charge increases the further the surrounding environment is from pI [8]. Therefore, a higher net protein molecule charge increases the electrostatic repulsion between the molecules, preventing the interactions required for gel matrix formation [5, 6]. This delays the association process between protein molecules, increasing the protein gel transparency and intricacy due to the sufficient precedence of protein aggregate ordering.

Muscle protein oxidation generally occurs during the processing and storage of meat and meat products, mainly due to the presence of metal ions, myoglobin, and fat oxidation products. Oxidation causes main protein chain (peptide bond) breakage, amino acid side chain modification, and covalent protein molecule cross-linking, changing the functional characteristics of the protein, including gel, water retention, and emulsification properties [4, 6]. In the predominant factors causing protein oxidation in meat and meat products, such as lipid oxidation, metmyoglobin oxidation, and hydroxyl radical oxidation, the •OH radical is the most reactive free radical of oxygen and is primarily produced by the Fenton reaction [9]. Therefore, hydroxyl radical-mediated protein oxidation is generally studied to investigate the structural modifications and functional property changes of MP in meat products.

Due to the unique geographical environment, biochemical yak meat components may differ significantly from other species [10]. Yak meat is low fat and protein-rich compared to cattle [11]. Although many studies have suggested that the oxidation of different protein types during food processing and storage significantly impacts the protein gel properties, minimal research is available regarding the effect of protein oxidation on the heat-induced gel properties of yak MP. Therefore, examining the influence of oxidative modification on the thermal aggregation characteristics of yak MP can reveal the underlying mechanism. This study assesses the impact of protein oxidation of Fenton system-derived hydroxyl radicals on the gel characteristics and thermal aggregation of yak MP and explores the relationship between the gel properties and the protein structure.

Materials and methods

Materials

Frozen (-20 °C) yak meat, 8 kg was purchased from Natural Ranch in Hongxian, SiChuan, China. Samples were packed in a vacuum bag in -20℃ refrigerator and brought to the laboratory. Ethylene glycol bis(2-aminoethyl)tetraacetic acid (EGTA), 2,4-Dinitrophenylhydrazine, 1,8-ANS, and glutaraldehyde were purchased from Chengdu Cologne Chemical Co. Ltd, Sichuan, China.

MP extraction

The MP was extracted from the *longissimus dorsi* yak muscle using a method described by Zheng [12]. The final MP was stored at 4 ℃ and used within 48 h. The protein concentration was determined via the Biuret method, using bovine serum albumin as a standard [2, 9].

MP oxidation

The MP (5 mg/mL) was oxidized(5 mmol/L, 10 mmol/L, 15 mmol/L, 20 mmol/L, 40 mmol/L, and 60 mmol/L) using a method delineated by Xiong et al. [13] with slight modifications. The MP solution (dissolved in 15 mmol/L PIPES buffer, pH 6.0) was dispersed in a Fenton oxidation system at a serial H_2O_2 concentration (0.6 mol/L NaCl, 0.01 mmol/L $FeCl_3$, 0.1 mmol/L ascorbic acid, and 5 mmol/L, 10 mmol/L(Low oxidation environment), 15 mmol/L, 20 mmol/L(Medium oxidizing environment), 40 mmol/L, and 60 mmol/L(High oxidation environment) H_2O_2, respectively), and incubated via continuous shaking in air in the dark at 4 ℃ for 24 h. The final pH levels were adjusted to 5.0, 6.0, 7.0, and 8.0(Acidic, neutral, alkaline environment), respectively, using NaOH or HCl. EDTA (1 mmol/L, final concentration) was added to terminate the oxidation process. The protein solution was dialyzed with deionized water at 4 ℃ for 72 h to remove the residual action agent, followed by lyophilization and storage at 4 ℃. The control group used deionized water instead of H_2O_2.

MP gel Preparation

The MP (40 mg/mL) was dissolved in a 1 mM phosphoric acid buffer solution (containing 0.6 mol/L NaCl) with serial pH values (pH 5.0, 6.0, 7.0, and 8.0), after which the protein concentration was adjusted to 40 mg/mL. Each protein solution sample (20 mL and 5 mL, respectively) was placed in a sample bottle and sealed with a flip-top rubber plug. The bottles were heated from 25 ℃ to 80 ℃ in a water bath, which was maintained for 20 min for gel

formation. The gel was cooled in an ice water bath and stored overnight in a 4 ℃ refrigerator for subsequent textural, whiteness, and scanning electron microscopy measurements.

Carbonyl content

The carbonyl content was determined using 2,4-dinitrophenylhydrazine (DNPH) according to a method described by Jia [14]. Here, 1 mL of MP solution at a concentration of 4 mg/mL was placed in a 10 mL centrifuge tube, after which 1 mL of 10 mmol/L 2,4-dinitrophenylhydrazine (the solvent is 2 mol/L hydrochloric acid) was added. The solution was left to react in the dark at 20 ℃ for 1 h (shaking every 15 min), after which a 1 mL 20% trichloroacetic acid (TCA) solution was added and centrifuged at 12,000 ×*g* for 5 min. The supernatant was discarded, and the precipitate was washed three times with 1 mL of ethyl acetate: ethanol (1:1, V: V). Then, 4 mL of a guanidine hydrochloride solution(6 mol/L) was added to the precipitate and dissolved in a water bath at 37 ℃ for 15 min. After adding the reaction solution, the mixture was centrifuged at 12,000 ×*g* for 3 min to remove insoluble substances, after which the UV absorbance of the supernatant was measured at 370 nm. The carbonyl content was calculated using a molecular absorbance coefficient of 22,000 [L/(mol • cm)], expressed as nmol/mg protein:

$$Carbonyl = \frac{A}{C * D * 22000} * 10^6 * n$$

A is the absorbance value of the sample, C is the MP concentration, D is the colorimetric optical path, and n is the dilution factor.

Protein solubility

The MP sample solution at a final 1 mg/mL concentration was centrifuged at 10,000 ×*g* for 10 min. The soluble protein concentration was determined via the biuret method using bovine serum albumin(BSA) as a standard. The protein solubility was expressed as the ratio of the protein in the supernatant to the total protein in the aqueous protein solution [5].

Surface hydrophobicity

The surface hydrophobicity of the MP samples was determined via a technique delineated by Jian Huajun [15], using 1-phenylaminonaphthalene-8-sulfonic acid as a fluorescence probe. The 1-phenylaminonaphthalene-8-sulfonic acid emitted minimal fluorescence in an aqueous environment, increasing significantly in a hydrophobic setting. Therefore, the fluorescence intensity (FI) variation of the 1-phenylaminonaphthalene-8-sulfonic acid probe reflected the hydrophobicity changes in the surrounding microenvironment since the 1-phenylaminonaphthalene-8-sulfonic acid tended to combine with the protein hydrophobic region. The FI was measured using a fluorescence photometer (F-4700, Japan's Nako Office) at an excitation wavelength of 374 nm and an emission wavelength of 484 nm. The initial slope of the FI and protein concentration plot was calculated via linear regression analysis and used as an index for protein hydrophobicity.

Intrinsic fluorescence

The endogenous fluorescence spectrum of the protein was determined using a method delineated by Jiang et al. [16]. with minor modifications. The MP concentration was adjusted to 0.5 mg/mL using a phosphate buffer solution (20 mmol/L, pH 5.0, 6.0, 7.0, and 8.0) corresponding to the pH value of the protein solution. The tryptophan fluorescence spectrum was measured at an excitation wavelength of 295 nm and an emission wavelength of 300–400 nm using a fluorescence photometer (ASD Field Spec Pro FR, Boulder Corporation, USA).

Secondary structure (fourier-transform infrared spectroscopy)

The freeze-dried protein samples were mixed with KBr and ground. They were then examined via Fourier infrared spectroscopy (ASD Field Spec Pro FR, American Boulder, Inc.) using a technique described by Kang [17], with slight modifications. The samples were scanned in a range of 400–4000 cm^{-1} at a resolution of 4 cm^{-1}. The PeakFit 4.0 software was used to analyze the data from 1600 cm^{-1} to 1700 cm^{-1} for Gaussian fitting. The relative secondary MP structure percentages were determined using the individual integrated sub-peak areas.

Rheological MP gel

The dynamic rheological properties of the MP gel were measured using a rheometer(DISCOVERY HR-1 Rotational Rheometer, TA Instruments in United States). The gel samples were placed between the parallel plate (25 mm radius, 1 mm gap), covered with a cap, and sealed with silicone oil to prevent moisture evaporation during the procedure. The temperature was scanned from 25°C-80°C at a rate of 1°C min^{-1} and a constant oscillation frequency of 1.0 Hz. The elastic modulus G' change during the heating process was measured [18].

Characteristic of MP gel

Gel strength

The textural properties of the protein gel were determined using a texture analyzer (TA.XT-Plus, Stable Micro Systems) with P/50 and P5 probes (5 mm in diameter). The pre-test and post-test speed was 10 mm/s, while the test speed was 0.5 mm/s. The pushing distance

was 10 mm, and the trigger force was 5 g. The maximum sustained compression force was described as the gel strength(g).

Water-holding capacity (WHC)

The WHC was determined using a method delineated by Delles et al. [19]. Gel samples with M_1 weights were packed with filter paper. After centrifugation at 4000 g for 10 min at 4 ℃, the gel presented M_2 weights. The WHC was defined using the following equation: $WHC = \frac{M_2}{M_1} \times 100\%$

Microstructure (SEM)

The gel was sampled and fixed using methods described by Han Minyi [20]. The gel samples were cut into 5-mm (1 cm*1 cm) cubes and fixed with 2.5% glutaraldehyde in a 0.1 M phosphoric acid buffer solution (pH 7.3) at 4 ℃ for 24 h. After 3-min rinses with cold a 0.1 M sodium phosphate solution (pH 7.3), 2.5% glutaraldehyde in a 0.1 M phosphoric acid buffer solution (pH 7.3) was used for secondary fixation at 4 ℃. Next, the samples were washed three times for 3 min with a 0.1 M phosphoric acid buffer solution (pH 7.0), followed by 15-min dehydration cycles with 50, 70, 80, and 90% ethanol solution, respectively. Finally, it was dehydrated by soaking in ethanol (100%) for 3 times consecutively. The freeze-dried samples were affixed to the sample table with double-sided tape and sputter-coated with approximately 10 nm thick gold film using an ion sputtering instrument. Three fields of each sample were observed using a scanning electron microscope (Thermo Scientific Apreo 2 C, Seymour fly).

Intermolecular interaction

The hydrophobic interactions, ionic bonds, disulfide bonds, and hydrogen bonds were measured at different pH values (5.0, 6.0, 7.0, and 8.0) using methods delineated by Nina [21]. Here, 2 g protein gel samples were placed in five test tubes, followed by the addition of 10 mL of five solutions: SA (0.05 mol/L NaCl), SB (0.6 mol/L NaCl), SC (0.6 mol/L NaCl + 1.5 mol/L urea), SD (0.6 mol/L NaCl + 8.0 mol/L urea), SE (0.6 mol/L NaCl + 8.0 mol/L urea + 0.05 mol/L β-Mercaptoethanol), respectively. The samples were homogenized at 5,000 rpm for 2 min. The subsequent homogenates were stirred at 4 ℃ for 60 min and centrifuged at 10,000 g for 15 min. The protein content of the supernatant was determined using the Biuret method. The intermolecular forces were defined using the following equation:

$$Ionic\ bond = protein\ content\ of\ SB\ sample - protein\ content\ of\ SA\ sample$$

$$Hydrogen\ bond = protein\ content\ of\ SC\ sample - protein\ content\ of\ SB\ sample$$

$$Hydrophobic\ interaction = protein\ content\ of\ SD\ sample - protein\ content\ of\ SC\ sample$$

$$Disulfide\ bond = protein\ content\ of\ SE\ sample - protein\ content\ of\ SD\ sample$$

Statistical analysis

The data were analyzed using Statistics software (SPSS 25.0, Chicago, IL, USA). All data were expressed as the means ± standard deviation. The significant differences ($p < 0.05$) between the means were identified via Duncan's multiple-range tests. All experiments were performed in triplicate. The figures were plotted using Origin 8.5.

Results and discussion

Carbonyl content

The degree of protein oxidation can be expressed by changes in carbonyl content [17]. As shown in Table 1, the carbonyl content of yak MP increased significantly ($p < 0.05$) at a higher H_2O_2 concentration. The main and side chain groups of the protein were primarily oxidized via free radicals, which converted the main peptide chain and aliphatic amino acid side chain groups into protein alkoxy radicals via hydrogen abstraction, oxygenation, hydrogenation, and single electron reduction [22]. The alkoxy radicals of the main polypeptide chain can undergo cleavage by either α-amidation or the diamine pathway to produce a large number of carbonyl groups [23]. The alkyl oxygen free radicals of the aliphatic amino acid side chain are directly decomposed into carbonyl compounds, breaking the protein peptide chain. Carbonyl compounds can also form directly via molecular rearrangement to increase the carbonyl content [24]. Therefore, the carbonyl content is generally used as an indicator to measure the degree of protein oxidation. The

Table 1 The effect of different H_2O_2 concentrations (mmol/L) on the MP carbonyl content (nmol/mg) at pH value

H_2O_2 concentration (mmol/L)	pH values			
	5	6	7	8
0	2.73 ± 0.15^{Da}	2.71 ± 0.25^{Da}	2.70 ± 0.40^{Da}	2.72 ± 0.20^{Da}
5	4.43 ± 0.18^{Cb}	4.17 ± 0.35^{CDb}	3.64 ± 0.35^{Ca}	3.97 ± 0.27^{CDa}
10	5.29 ± 0.16^{BCb}	4.91 ± 0.10^{BCb}	4.41 ± 0.15^{BCa}	4.22 ± 0.30^{BCa}
15	5.93 ± 0.21^{ABCc}	5.47 ± 0.30^{ABb}	4.94 ± 0.23^{BCa}	4.76 ± 0.40^{BCa}
20	6.49 ± 0.30^{ABCc}	6.13 ± 0.40^{ABb}	5.69 ± 0.31^{Ba}	5.47 ± 0.16^{BCa}
40	7.44 ± 0.10^{ABc}	6.65 ± 0.50^{Ab}	6.13 ± 0.40^{Aa}	6.02 ± 0.135^{Ba}
60	7.98 ± 0.15^{Ac}	7.04 ± 0.18^{Ac}	6.64 ± 0.28^{Aa}	6.52 ± 0.215^{Ab}

$^{A–G}$ Different letter within the same column indicate statistically different ($p < 0.05$)

$^{a–d}$ Different letter within the same row indicate statistically different ($p < 0.05$)

carbonyl content concentration at higher oxidant concentrations was considerably lower at pH 7.0(6.64) and 8.0(6.52) than at pH 5.0(7.98) and 6.0(7.04), indicating that the MP was more vulnerable to ·OH attack near the pI at the same oxidant concentrations. That's because the stability of the protein structure is decreased near pI, and the α-helical structure was mostly converted to β-sheet, protein becomes at the dispersed state, protein is more susceptible to ·OH attack [17].

Solubility

Protein solubility is mainly affected by the interaction between protein molecules (such as hydrophobic interaction and disulfide bonds) and protein-water interaction (such as ion-dipole and dipole-dipole) [25]. The protein solubility increases as the protein-water interaction improves and decreases with enhanced protein-protein interaction [9, 10]. Table 2 shows the changes in the MP solubility when exposed to different treatments. At the same oxidant concentrations, the protein solubility increased significantly at a higher pH ($p < 0.05$),when the pH is increased from 5.0 to 8.0, the solubility increases by 30%. No electrostatic repulsion was evident between the protein molecules due to a lower net charge near the MP pI (about 5.3), which enhanced the protein-protein contact due to hydrophobic interaction, leading to protein aggregation or precipitation. The approach of protein molecules causes intermolecular cross-linking via protein oxidation. Oxidation aggravated the degree of insoluble protein aggregation, causing a higher MP solubility loss at pH 5.0 than that at other pH levels, as shown in Table 2. A pH far from the pI increased the negative MP charge, and reduced the interaction between the electrostatic repulsion molecules. In the same pH conditions, higher H_2O_2 concentrations significantly decreased the MP solubility compared with the control group ($p < 0.05$). This was mainly due to the covalent cross-linking caused by protein oxidation, forming insoluble aggregates. The protein solubility decreased further as the number of insoluble aggregates increased with the degree of oxidation [26].

Table 2 The solubility of the MP treated with H_2O_2 concentrations at different pH levels(%)

H_2O_2 concentration (mmol/L)	pH values			
	5	6	7	8
0	21.33 ± 0.25^{Ad}	22.99 ± 0.54^{Ac}	32.90 ± 0.25^{Ab}	33.59 ± 0.3^{Aa}
5	20.29 ± 0.3^{Bd}	20.84 ± 0.58^{Bc}	30.96 ± 0.50^{Bb}	32.76 ± 0.19^{Ba}
10	19.45 ± 0.48^{Cd}	20.56 ± 0.47^{Cc}	28.46 ± 0.32^{Cb}	31.31 ± 0.65^{Ca}
15	17.65 ± 0.35^{Dd}	19.87 ± 0.2^{Dc}	27.56 ± 0.35^{Db}	31.24 ± 0.23^{Ca}
20	17.24 ± 0.52^{Ed}	19.45 ± 0.32^{Ec}	25.69 ± 0.52^{Eb}	29.43 ± 0.4^{Da}
40	14.47 ± 0.3^{Fd}	19.32 ± 0.25^{Ec}	25.28 ± 0.3^{Fb}	29.16 ± 0.23^{Ea}
60	12.33 ± 0.35^{Gd}	17.21 ± 0.5^{Fc}	24.44 ± 0.43^{Gb}	27.94 ± 0.34^{Fa}

$^{A–G}$ Different letter within the same column indicate statistically different ($p < 0.05$)

$^{a–d}$ Different letter within the same row indicate statistically different ($p < 0.05$)

Surface hydrophobicity

Surface hydrophobicity is used to evaluate the changes in chemical and physical protein states [27]. The hydrophobic amino acid content on the protein surface reflects the degree of protein denaturation and hydrophobic force [28]. As shown in Table 3, in series pH conditions, the protein surface hydrophobicity increased significantly compared with the control group at a higher oxidant concentration ($p < 0.05$), with a growth rate of about 26.2%(pH 5.0), 29.5%(pH 6.0), 25.0%(pH 7.0), 21.8%(pH 8.0) (growth rate = Surface hydrophobicity(O_{60}-O_0)/O_0). The naturally folded structures of native MPs contain hydrophobic residues, especially non-polar aromatic amino acids, with fewer hydrophobic groups, consequently reducing the surface hydrophobicity. Higher surface hydrophobicity indicated a change in the spatial structures of the MP molecules, causing MP unfolding and exposure of the buried hydrophobic groups. This caused irreversible protein denaturation after aggregate formation due to hydrophobic interaction. In addition, oxidation modified the amino acid residues on the globulin surface, resulting in complex surface hydrophobicity changes [5]. The hydrophobic side chains of Met were converted into hydrophilic groups. Lys ε-NH_2 oxidation to electroneutral carbonyl derivatives reduced the

Table 3 The effect of H_2O_2 concentrations at different pH levels on the surface hydrophobicity of the Yak meat MP

H_2O_2 concentration (mmol/L)	pH values			
	5	6	7	8
0	383.64 ± 7.12^{Fa}	285.58 ± 4.20^{Gb}	245.21 ± 4.12^{Ec}	238.99 ± 4.51^{Ed}
5	425.37 ± 3.10^{Ea}	298.2 ± 4.38^{Fb}	268.71 ± 4.61^{Dc}	241.72 ± 2.26^{Ed}
10	427.01 ± 8.55^{Da}	310.6 ± 2.67^{Eb}	270.21 ± 7.11^{CDc}	252.52 ± 6.39^{Dd}
15	430.81 ± 9.25^{Ca}	335.19 ± 11.03^{Db}	272.79 ± 3.12^{Cc}	271.1 ± 1.70^{Cc}
20	455.26 ± 3.18^{Ba}	345.24 ± 15.43^{Cb}	282.05 ± 1.01^{Bc}	276.09 ± 4.29^{Cd}
40	455.49 ± 7.10^{Ba}	358.42 ± 5.08^{Bb}	285.71 ± 2.25^{Bc}	283.64 ± 3.41^{Bc}
60	484.23 ± 5.34^{Aa}	369.92 ± 6.63^{Ab}	306.69 ± 2.78^{Ac}	291.13 ± 3.41^{Ad}

$^{A–G}$ Different letter within the same column indicate statistically different ($p < 0.05$)

$^{a–d}$ Different letter within the same row indicate statistically different ($p < 0.05$)

positive charge, decreasing the hydrophilicity. Furthermore, the Michael addition between Lys, Cys, and His and lipid oxidation products α- and β-unsaturated aldehydes caused long-chain alkanes to attach to the protein side chains, increasing the hydrophobicity [29]. The surface hydrophobicity of the MP treated with oxidant (pH 5) was significantly higher than in the other groups ($p < 0.05$). Oxidized protein unfolding may outweigh aggregation, increasing the surface hydrophobicity. A higher pH increased the intermolecular repulsion force, reduced the aggregation behavior of proteins driven by hydrophobic interaction, and decreased the hydrophobicity [26].

Intrinsic fluorescence

The loss of intrinsic tryptophan fluorescence typically indicates conformational protein change [30]. As the oxidant concentration increased, a wavelength blue shift occurred in the λmax emission of each group, from the initial 342 nm to 339 nm, accompanied by intrinsic FI loss, compared to the control sample (Fig. 1). Tryptophan displays the lowest single electron oxidation potential of protein amino acids. It is sensitive to ·OH and is easily oxidized into tryptophan free radicals. It combines with molecular oxygen to form tryptophan peroxidative free radicals and, ultimately kynurenine, decreasing endogenous FI [31]. The λmax is related to the tryptophan microenvironment. When tryptophan residues are transferred from an aqueous to a hydrophobic setting, their

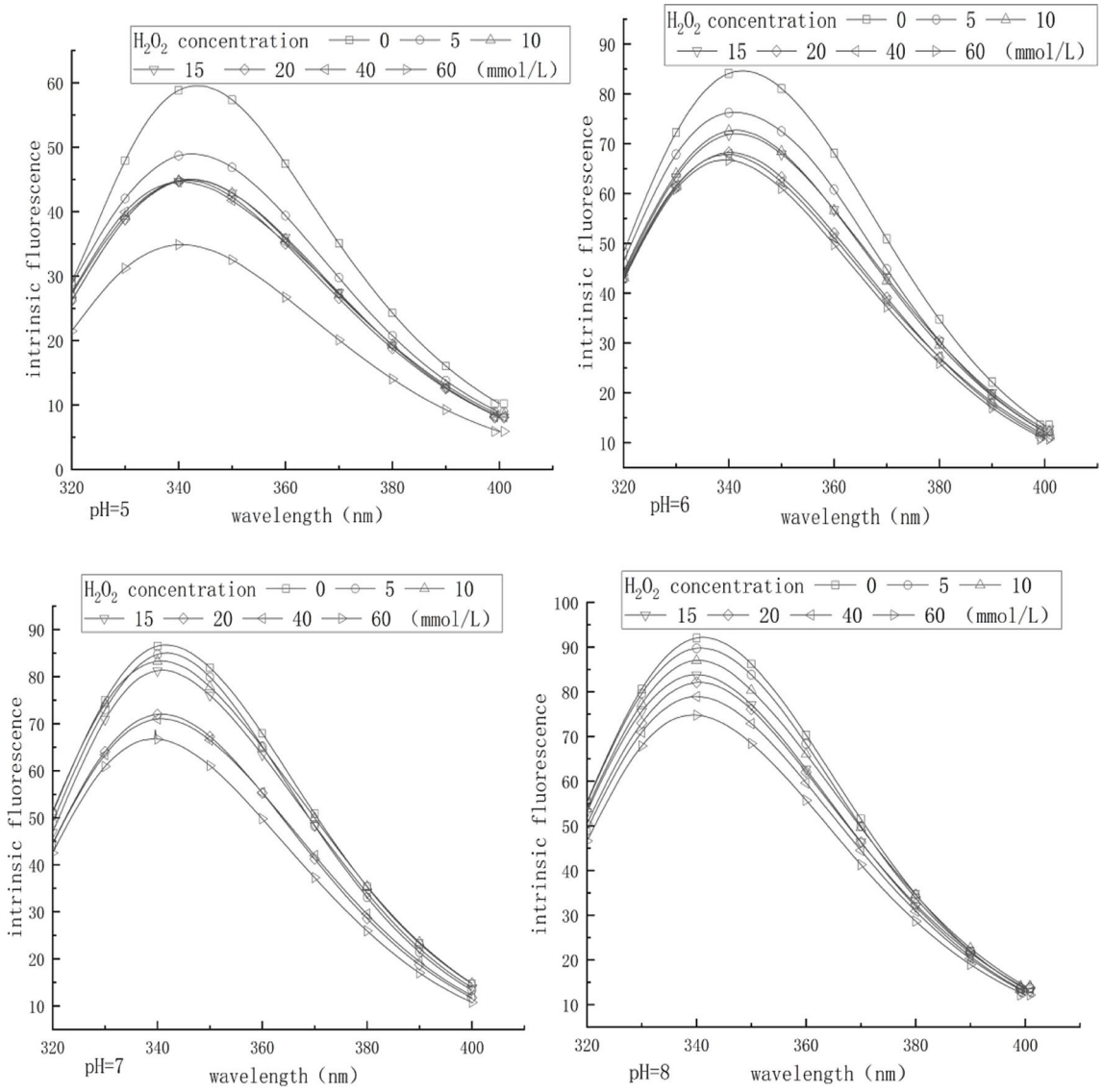

Fig. 1 The effect of series H_2O_2 concentrations at different pH levels on the intrinsic MP fluorescence. Significant differences are evident between the treatment groups regarding blue shift and intrinsic FI loss ($P < 0.05$)

fluorescence spectra experience a blue shift, while a red-shift occurs during transference from a hydrophobic to an aqueous environment [25]. The Trp fluorescence spectra blue shift indicated that the initially exposed tryptophan residues in the MP were embedded in the oxidized MP aggregates due to protein aggregation [32]. At high oxidant concentrations, the intrinsic FI loss was significantly higher in the pH 5.0 group than in the other pH groups ($p < 0.05$), indicating the destruction of more tryptophan by oxidation near the pI. This confirmed that the MP near the pI was more vulnerable, which was consistent with the carbonyl content results. The pH alteration induced the different electronic configurations of the aromatic compound molecules or ions, leading to different FIs [33]. The Trp FI varied at each pH value.

Secondary structure (FT-IR)

The main peptide chain breakage and covalent cross-link formation caused by protein oxidation is always accompanied by internal protein structural changes [34, 35]. Since proteins display characteristic absorption bands in the infrared region that reflect changes in the functional groups of protein structures, FT-IR was used to detect structural changes after oxidation. The relative content of the various secondary structural elements in the yak muscle MP, α-helices, β-sheets, β-turns, and random coils were calculated and listed in Table 4. Higher H_2O_2 concentrations at the same pH values significantly increased the random coils($p < 0.05$), suggesting a substantial decline in the total secondary structure proportion of the oxidant-treated MP. The β-sheets increased significantly ($p < 0.05$), while the α-helices and β-turns displayed a substantial decrease ($p < 0.05$). The secondary structure decline could be attributed to the unfolding of the protein molecule structure and the exposure of the buried groups. Furthermore, reactive oxygen species changed the secondary protein structure by weakening the hydrogen bonds [36]. Therefore, the MP α-helices gradually unfolded, rearranging the polypeptide chain to form β-sheets. At the same oxidant concentration, the oxidant-treated MP at pH 5.0 and pH 6.0 presented more β-sheets and fewer α-helices than the pH 7.0 group.

Rheological properties

The G' typically represents elasticity and reflects the different stages of protein unfolding and aggregation, as well as gel strength. Figure 2 shows the G' changes in the yak meat MP gel after different oxidation treatments. The G' values of all the gel samples were relatively stable during the initial low-temperature heating stage. Subsequently, the G' showed three gelation phases during the heating process after 45 ℃ at pH 6.0, 7.0, and 8.0. This rheological transition was widely observed during MP and myosin gelation, evidenced by the stepwise structural changes

Table 4 Effects of H_2O_2 concentrations on the secondary structure of MP at different pHs(transmittance)

H_2O_2 (mmol/L)	β - Folding				No regular curl				α- Helix				β - corner			
	5	6	7	8	5	6	7	8	5	6	7	8	5	6	7	8
0	31.59 ± 0.83^{Da}	27.29 ± 0.94^{Db}	24.82 ± 0.48^{Dc}	26.55 ± 0.77^{Dc}	14.39 ± 0.08^{Eab}	15.60 ± 0.51^{Eb}	16.95 ± 1.08^{Eab}	13.72 ± 0.69^{Ea}	18.94 ± 0.66^{Ac}	20.28 ± 1.05^{Ac}	25.37 ± 1.32^{Ab}	24.14 ± 0.43^{Aa}	34.92 ± 0.65^{Aa}	34.21 ± 0.22^{Aa}	36.82 ± 1.05^{Aa}	34.41 ± 0.74^{Ab}
5	32.15 ± 0.31^{Da}	30.00 ± 1.07^{DCb}	26.85 ± 0.54^{DCc}	27.64 ± 0.72^{DCc}	17.71 ± 1.02^{Dab}	16.63 ± 0.79^{Db}	17.97 ± 0.87^{Dab}	18.43 ± 0.60^{Da}	18.02 ± 0.17^{Bc}	18.73 ± 0.77^{Bc}	23.56 ± 0.90^{Bb}	22.79 ± 1.13^{Ba}	31.69 ± 0.64^{Ba}	32.96 ± 0.46^{Ba}	34.02 ± 0.73^{Ba}	30.69 ± 0.94^{Bb}
10	34.72 ± 0.95^{BCa}	30.91 ± 1.10^{BCb}	27.15 ± 0.19^{BCc}	28.55 ± 0.14BCc	18.13 ± 0.99^{CDab}	18.18 ± 0.50^{CDb}	18.14 ± 0.95^{CDab}	20.30 ± 1.79^{CDa}	17.82 ± 1.03^{Cc}	16.34 ± 1.09^{Cc}	22.94 ± 0.29^{Cb}	21.86 ± 0.61^{Ca}	31.64 ± 0.52^{BCa}	31.74 ± 1.04^{BCa}	33.13 ± 1.32^{BCa}	28.63 ± 0.56^{BCb}
15	35.13 ± 0.81^{BCa}	31.06 ± 0.50^{BCb}	27.53 ± 0.68^{BCc}	28.87 ± 0.46^{BCc}	19.26 ± 1.03^{BCab}	19.62 ± 0.73^{BCb}	20.02 ± 0.58^{BCab}	21.95 ± 1.94^{BCa}	16.77 ± 0.77^{CDc}	16.21 ± 0.55^{CDc}	21.55 ± 0.40^{CDb}	20.64 ± 0.57^{CDa}	31.23 ± 1.13^{BCa}	31.29 ± 0.37^{BCa}	32.15 ± 0.89^{BCa}	26.71 ± 0.38^{BCb}
20	35.52 ± 0.57^{Ba}	32.28 ± 1.13^{Bb}	28.39 ± 0.61^{Bc}	29.36 ± 0.22^{Bc}	20.61 ± 0.82^{Bab}	19.90 ± 1.05^{Bb}	20.55 ± 0.68^{Bab}	22.94 ± 0.11^{Ba}	15.48 ± 0.99^{Dc}	15.42 ± 0.45^{Dc}	21.02 ± 0.66^{Db}	19.83 ± 0.42^{Da}	30.39 ± 0.21^{CDa}	30.69 ± 0.49^{CDa}	31.69 ± 0.62^{CDa}	26.13 ± 0.87^{CDb}
40	36.98 ± 0.68^{Aa}	37.04 ± 0.15^{Ab}	29.02 ± 0.63^{Ac}	30.44 ± 0.49^{Ac}	22.59 ± 0.24^{ABab}	20.42 ± 0.66^{ABb}	21.25 ± 1.01^{ABab}	23.08 ± 0.91^{ABa}	14.41 ± 0.72^{Ec}	15.10 ± 0.91^{Ec}	20.27 ± 1.11^{Eb}	17.21 ± 1.21^{Ea}	29.77 ± 0.43^{DEa}	30.29 ± 0.72^{DEa}	27.30 ± 0.88^{DEa}	24.84 ± 0.99^{DEb}
60	39.22 ± 0.78^{Aa}	38.84 ± 0.62^{Ab}	30.95 ± 0.78^{Ac}	31.05 ± 0.64^{Ac}	26.64 ± 0.05^{Aab}	21.55 ± 0.54^{Ab}	22.44 ± 1.42^{Aab}	24.19 ± 1.16^{Aa}	13.82 ± 0.88^{Ec}	13.62 ± 0.46^{Ec}	19.80 ± 0.69^{Eb}	15.37 ± 0.08^{Ea}	28.45 ± 0.51^{Ea}	27.70 ± 0.73^{Ea}	24.89 ± 0.56^{Ea}	22.97 ± 0.96^{Eb}

$^{A-E}$.Different letter within the same column indicate statistically different ($p < 0.05$)

$^{a-c}$ Different letter within the same row indicate statistically different ($p < 0.05$)

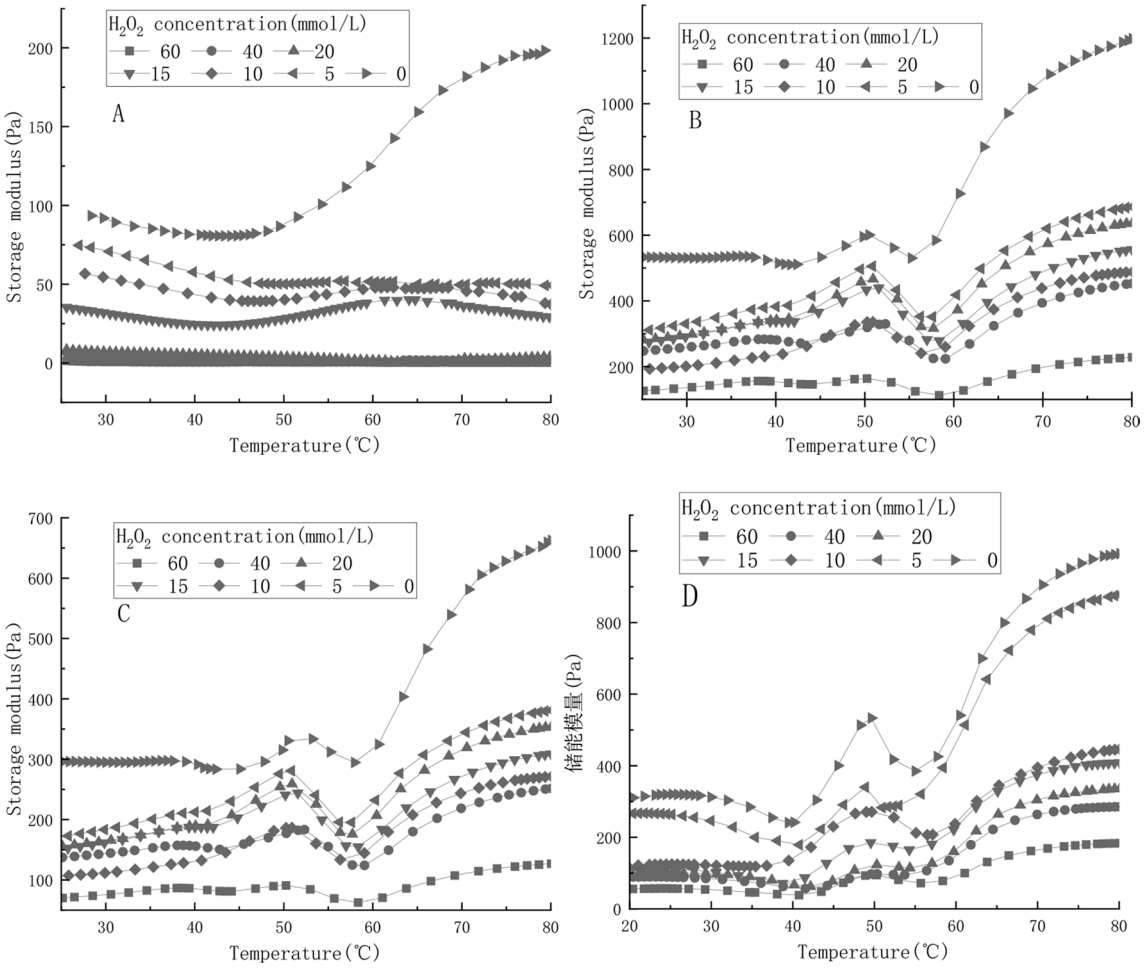

Fig. 2 Changes in storage modulus (G') changes of MP gels after treating with different H_2O_2 concentrations at pH 5 (**A**), pH 6.0 (**B**), pH 7.0 (**C**), and pH 8.0 (**D**)

and interaction between MPs, notably myosin. Except for the pH 5.0 group, a higher G' was evident as the temperature increased from 45 ℃ to 50 ℃, with the first peak at about 50 ℃. Yan et al. showed that the denaturation and dissociation resulting from hydrogen and disulfide bond cleavage were accompanied by hydrophobic interaction and disulfide bond association [32]. Dissociation MP decreased the G', while association increased this value. The flat plateau region of the MP G' suggested the absence of dissociation or association. Furthermore, no gel structure formation was evident during the initial heating stage. During the post-heating phase, the initial increase was attributed to heavy meromyosin unfolding and myosin head cross-linking, resulting in a weak gel structure [35]. The rapid aggregate formation and prominent G' increase were mainly attributed to enhanced hydrophobic interactions as the temperature rose. After declining dramatically to a minimum at 58 ℃ in the pH 6.0, 7.0, and 8.0 groups, the G' increased steadily after subsequent heating. Xiong et al. [12]indicated that the rheological transition (peak) could be ascribed to initial myosin head association due to S1 subfragment denaturation (42 ℃ to 48 ℃) and the temporary protein network disruption due to subsequent myosin tail unfolding (the rod subfragment) (50 ℃ to 55 ℃). The peak G' values of all the groups declined gradually as the oxidant concentrations increased, suggesting that oxidation cross-linking and aggregation in MP occurred prior to denaturation and dissociation, decreasing thermal protein polymerization. During the third phase (58°C to 85°C), the rapid G' increase reflected the formation of a strong, tight three-dimensional structure via protein cross-linking and aggregation. Oxidation markedly decreased the G' over the entire temperature range in all the pH groups as the MP was converted into a gel, suggesting that the protein oxidation weakened the three-dimensional network structure of MP gels. This was consistent with the gel strength results. Since oxidation was highest as the MP neared the pI, the gel structure was distorted so severely that no peaks appeared in the G' curve, while the G' value was lowest in the pH 5.0 group.

Table 5 Effects of H_2O_2 concentrations on the gel strength of the Yak MP gel at different pH levels

H_2O_2 concentration (mmol/L)	pH values			
	5	6	7	8
0	53.46 ± 0.74^{Ac}	61.46 ± 0.50^{Aa}	58.62 ± 0.93^{Ab}	57.16 ± 0.94^{Ab}
5	51.01 ± 0.27^{Bd}	59.77 ± 0.73^{Ba}	57.00 ± 0.33^{ABb}	55.54 ± 0.25^{Ac}
10	50.79 ± 0.67^{Bd}	58.41 ± 0.93^{BCa}	56.44 ± 0.92^{Bb}	53.64 ± 0.27^{Bc}
15	50.03 ± 0.29^{BCb}	57.97 ± 0.44^{Ca}	55.64 ± 0.77^{BCa}	52.24 ± 1.83^{BCb}
20	49.90 ± 0.54^{BCc}	56.79 ± 0.65^{CDa}	54.32 ± 0.56^{CDb}	50.01 ± 0.88^{CDc}
40	48.62 ± 0.52^{CDc}	55.67 ± 0.82^{DEa}	53.29 ± 0.75^{Db}	50.00 ± 0.65^{Dc}
60	47.28 ± 1.04^{Dc}	54.05 ± 1.14^{Ea}	50.86 ± 1.05^{Eb}	49.20 ± 0.70^{Dbc}

$^{A–E}$ Different letter within the same column indicate statistically different ($p < 0.05$)

$^{a–C}$ Different letter within the same row indicate statistically different ($p < 0.05$)

Table 6 Effects of H_2O_2 concentrations on the WHC of the Yak MP gel at different pH values

H_2O_2 concentration (mmol/L)	pH values			
	5	6	7	8
0.00	77.24 ± 0.18^{Ab}	79.23 ± 1.60^{Ab}	82.95 ± 1.52^{Aa}	83.94 ± 1.17^{Aa}
5.00	75.65 ± 0.96^{ABc}	78.84 ± 0.38^{Ab}	80.10 ± 1.33^{Bb}	82.42 ± 0.62^{ABa}
10.00	75.18 ± 1.27^{ABCc}	77.17 ± 1.55^{ABbc}	79.24 ± 1.06^{BCab}	81.10 ± 0.62^{Ba}
15.00	74.87 ± 1.61^{ABCc}	75.89 ± 0.86^{BCbc}	78.84 ± 0.81^{BCab}	80.82 ± 0.13^{BCa}
20.00	74.27 ± 1.70^{ABCb}	75.36 ± 0.95^{BCDb}	77.97 ± 1.09^{BCDa}	79.09 ± 0.25^{CDa}
40.00	73.46 ± 1.64^{BCb}	74.31 ± 1.39^{CDb}	76.27 ± 0.52^{CDab}	78.98 ± 0.40^{CDa}
60.00	72.05 ± 1.33^{Cc}	73.01 ± 0.77^{Dbc}	75.29 ± 0.63^{Dab}	77.54 ± 0.17^{Da}

$^{A–D}$ Different letter within the same column indicate statistically different ($p < 0.05$)

$^{a–c}$ Different letter within the same row indicate statistically different ($p < 0.05$)

Gel strength

Gel strength is a vital index that can reflect the texture and sensory quality of meat products [37]. Table 5 shows the gel strength of the yak meat MP gel. A higher H_2O_2 concentration in the same pH conditions significantly decreased ($p < 0.05$) the gel strength of the oxidant-treated MP. As the H_2O_2 concentration increased from 0 mmol/L to 60 mmol/L, the gel strength decreased by approximately 11%(pH 5.0),12%(pH 6.0),13%(pH 7.0),14%(pH 8.0) in each pH group compared with the unoxidized group. Wu et al. indicated that oxidative modification by peroxyl radicals decreased the disulfide content of soy protein [38]. Disulfide bonds are crucial for maintaining protein gel structure [39]. Oxidation induced covalent cross-linking between the MP molecules, causing degeneration and complete protein unfolding. This facilitated spherical aggregate and disordered gel structure formation, uneven pore distribution, and increased compactness, as observed via SEM. The gel strength of the MP samples was highest at pH 5.0 at the same oxidant concentrations since the MP near the pI was more vulnerable to ·OH attack.

WHC

The WHC indicates the protein water binding ability and is a crucial feature of heat-induced gels, commonly used to objectively assess meat product quality. Table 6 shows the WHC changes in the MP gels after different oxidation treatments. The WHC results were consistent with the gel strength findings. Higher H_2O_2 concentrations in the same pH conditions significantly decreased ($p < 0.05$) the gel WHC. Compared with the control sample, the WHC of each pH group decreased by about 6%(pH 5),8%(pH 6),9%(pH 7),7%(pH 8) when the H_2O_2 concentration reached 60 mmol/L. The molecular structural changes in the protein after oxidation disturbed the orderly MP aggregation during the gel process, adversely affecting the three-dimensional network structure of the gel, resulting in a looser structure and larger pores that reduced the WHC. Xia et al. [40] found that the oxidative modification of pork muscle MP by metal-catalyzed hydroxyl radicals significantly decreased the WHC. Xiong [13] suggested lower MP WHC decreased the protein solubility and sulfhydryl during protein oxidation. The yak meat MP gel displayed the lowest WHC at pH 5.0, which improved significantly at pH levels far from the pI, especially at pH 8.0.

Microstructure

The porosity and coarseness of the yak meat MP gels were observed via scanning electronic microscopy. Coarseness is typically used to evaluate the homogeneity of the formed protein aggregates, while porosity assesses the distribution sparseness of single-row aggregates. Figure 3 shows the three-dimensional network structure of the control samples and partial oxidant-treated samples, revealing distinctive differences between the various MP gels. The SEM micrographs showed that the

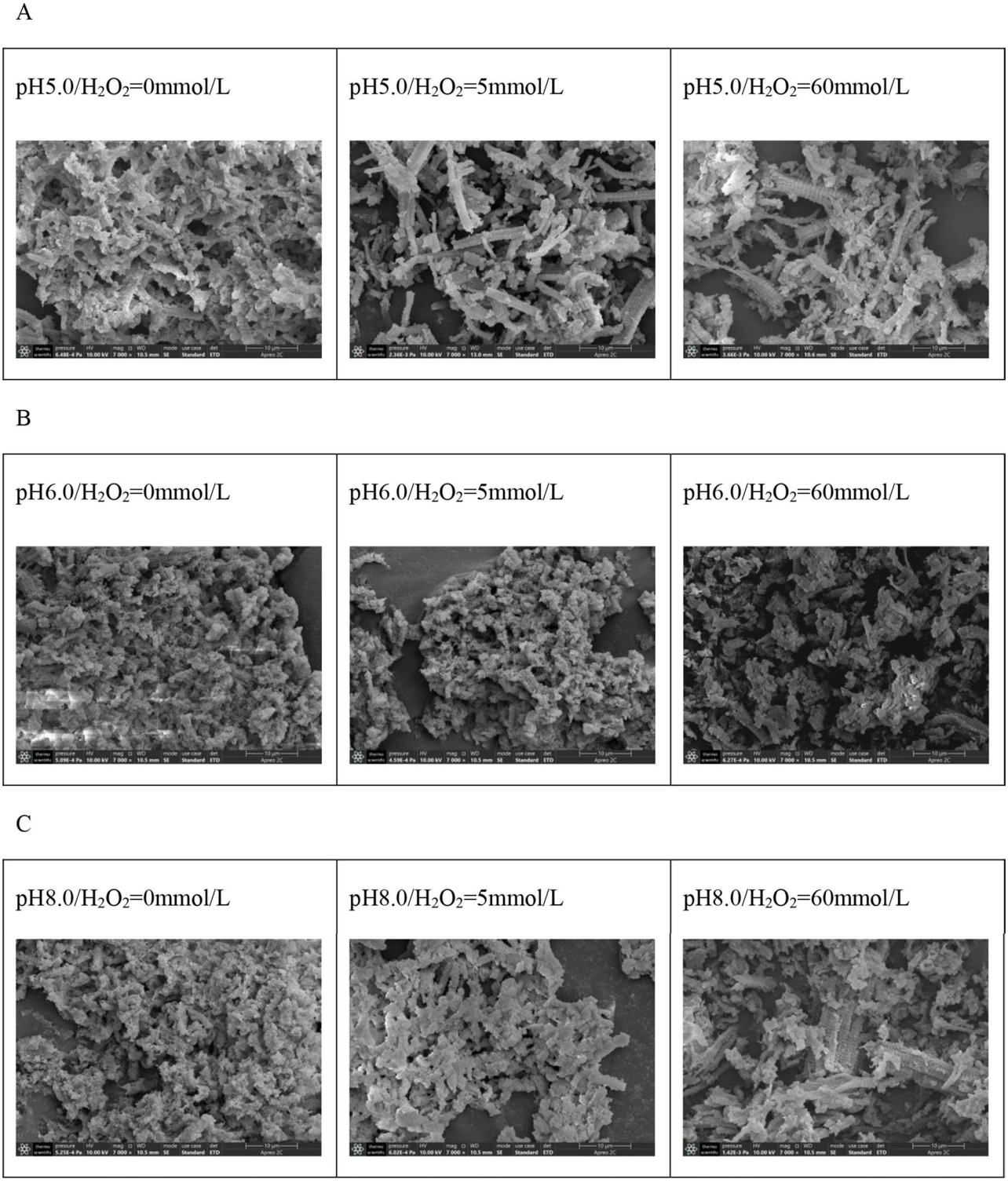

Fig. 3 The scanning electron microscopy micrographs of the MP gels after different oxidation treatments at 7000× magnification

untreated gel samples of three pH groups exhibited compacted networks with small, evenly distributed pores. The morphological characteristics of the MP gel structures were altered after protein oxidation with 5 mmol/L H_2O_2 (Fig. 3). The MP gel networks in all the pH groups appeared rough with large aggregates, forming a more continuous fibrous structure with many unevenly distributed pore voids and spaces. Further oxidative MP modification with 60 mmol/L H_2O_2 resulted in the formation of filamentous, irregular network structures with coarser,

Table 7 The influence of different H_2O_2 concentrations on the MP gel interaction at different pH levels

H_2O_2	Ionic bond				Hydrogen bond			
	5	6	7	8	5	6	7	8
0	0.035±0.001Ac	0.094±0.001Aa	0.085±0.003Ab	0.079±0.005Ab	0.074±0.002Ac	0.100±0.003Aa	0.094±0.007Ab	0.092±0.004Ab
5	0.032±0.002Ad	0.087±0.002Ba	0.073±0.003Bb	0.068±0.002Bc	0.064±0.004Bc	0.096±0.001ABa	0.092±0.003ABb	0.087±0.003ABb
10	0.024±0.002Bc	0.074±0.003Ca	0.066±0.003Cb	0.065±0.003BCb	0.055±0.001Cc	0.094±0.003BCa	0.086±0.007BCb	0.082±0.005BCb
15	0.02±0.001Bb	0.069±0.003CDa	0.063±0.004CDa	0.062±0.006Ca	0.047±0.005Dc	0.090±0.003CDa	0.085±0.003Cb	0.076±0.003Cb
20	0.016±0.004BCc	0.066±0.002DEa	0.059±0.007Db	0.053±0.003Db	0.040±0.003Ec	0.087±0.002Da	0.076±0.001Db	0.073±0.007Cb
40	0.011±0.001CDc	0.064±0.002DEa	0.052±0.002Eb	0.048±0.004Eb	0.037±0.004Ec	0.081±0.003Ea	0.073±0.002DEb	0.069±0.006Db
60	0.006±0.005Dc	0.061±0.002Ea	0.047±0.002Eb	0.041±0.004Fb	0.035±0.003Ec	0.075±0.009Fa	0.068±0.004Eb	0.063±0.004Db
H_2O_2	Disulfide bonds				Hydrophobic interactions			
	5	6	7	8	5	6	7	8
0	$0.629±0.057^{Dc}$	$1.395±0.028^{Ca}$	$0.827±0.010^{Cb}$	$0.877±0.084^{Cb}$	$1.591±0.022^{Ac}$	$3.383±0.083^{Fa}$	$3.118±0.051^{Eb}$	$2.385±0.027^{Fb}$
5	$0.642±0.026^{Dc}$	$1.405±0.032^{Ba}$	$0.886±0.080^{Bb}$	$0.904±0.061^{Bb}$	$1.752±0.038^{Bc}$	$3.623±0.029^{Ea}$	$3.360±0.064^{Db}$	$2.688±0.043^{Eb}$
10	$0.677±0.030^{Cc}$	$1.433±0.058^{ABa}$	$0.92±0.050^{Bb}$	$0.983±0.090^{Bb}$	$1.841±0.086^{CBc}$	$3.685±0.068^{DEa}$	$3.401±0.098^{CDb}$	$2.834±0.063^{Db}$
15	$0.755±0.011^{Cc}$	$1.459±0.056^{ABa}$	$0.945±0.012^{Bb}$	$0.996±0.064^{Bb}$	$1.876±0.022^{Cc}$	$3.751±0.073^{CDa}$	$3.451±0.061^{Cb}$	$2.920±0.051^{Cb}$
20	$0.786±0.045^{BCc}$	$1.556±0.021^{ABa}$	$0.953±0.012^{Bb}$	$1.086±0.064^{Ab}$	$1.893±0.080^{Cc}$	$3.764±0.024^{Ca}$	$3.641±0.025^{Bb}$	$3.029±0.054^{Bb}$
40	$0.825±0.014^{Bc}$	$1.569±0.044^{ABa}$	$0.997±0.041^{ABb}$	$1.118±0.025^{Ab}$	$2.073±0.090^{Bc}$	$3.879±0.032^{Ba}$	$3.736±0.065^{Ab}$	$3.090±0.060^{Bb}$
60	$0.922±0.020^{Ac}$	$1.606±0.054^{Aa}$	$1.097±0.035^{Ab}$	$1.153±0.032^{Ab}$	$2.395±0.034^{Ac}$	$4.000±0.039^{Aa}$	$3.773±0.083^{Ab}$	$3.195±0.009^{Ab}$

$^{A–F}$ Different letter within the same column indicate statistically different ($p < 0.05$), $^{a–c}$ Different letter within the same row indicate statistically different ($p < 0.05$)

inhomogeneous large pore distribution (Fig. 3). The microstructural formation in MP gels depends on the relative speed of protein aggregation and expansion. Slow aggregation is conducive to the full denaturation and expansion of protein molecules, forming highly extensible straight-chain molecules, slowly combining to form linear aggregates [41]. When the speed of globulin aggregation exceeded that of protein expansion, the oxidized protein cross-linking and aggregation occurred prior to total denaturation and unfolding, leading to spherical aggregate and disordered gel structure formation, uneven pore distribution, and increased compactness. The gel strength tests, WHC measurements, and rheological measurements indicated that the pH 5.0 group might exhibit more cross-linked strands due to oxidized protein aggregation. The protein gel displays the worst WHC and hardness at pH 5.0, optimal hardness at pH 6.0, and optimal WHC at pH 8.0. Therefore, the microstructures of the protein oxidation (5 mmol/L and 60 mmol/L) samples were observed at the three typical pH levels via scanning electron microscopy.

Intermolecular interaction

The stability of the three-dimensional protein gel structure is closely related to the chemical force, which requires the combined action of hydrophobic interaction, hydrogen bond, disulfide bond, ionic bond, and other forces [42]. As shown in Table 7, hydrophobic interaction represents the primary force for maintaining yak meat MP gel, followed by disulfide, hydrogen, and ionic bonds. A higher H_2O_2 concentration significantly decreased ($p < 0.05$) the ionic and hydrogen bond content while substantially increasing the disulfide bonds and hydrophobic interaction. This was mainly because ·OH-oxidized protein exposed the amino acid side-chain groups, which increased the protein hydrophobicity and hydrophobic interaction ($p < 0.05$). During oxidation, the charge group properties were modified, or the ionizable group underwent a chemical reaction, such as the Lys amino group, which reduced the ionic bonds. Furthermore, the secondary structure changes caused by oxidation weakened the hydrogen bond force [20]. At a higher H_2O_2 concentration, the sulfhydryl group of the cysteine side-chain was oxidized to form a disulfide bond, resulting in cross-linking and aggregation between the protein molecules [39] and increasing the disulfide bond content. Since the protein was near the pI at pH 5.0, the number of positive and negative charges carried by the protein molecules were basically equal, and the various forces between the proteins were lower than in the other pH groups, decreasing the textural hardness of the protein gel. pH deviation from the pI (pH 6.0) significantly increased the various protein interactions, which decreased as the pH level continued to rise. This may be because the protein surface charge further increases as the pH moves further away from the pI. The electrostatic repulsion force increases the distance between the protein molecules and the degree of protein hydration, reducing protein interaction.

Conclusion

Protein oxidation has a significant negative impact on the characteristics of yak meat MP gel. Myofibrillar protein (MP) determines the sensory properties, functional properties and nutritional quality of meat products. Metal ions, enzymes, ferrous heme and lipids in muscle are easy

to oxidize and produce reactive oxygen species, which can induce the oxidation of myofibrillar protein, thus affecting the gel properties, water retention and interfacial properties of meat products. In this study, a hydroxyl radical simulation system was established to explore the effects of different oxidation degrees at different pH on MP structure and gel properties of yak meat from the perspective of molecular structure, fully explore the mechanism and essence of protein oxidation, and provide a theoretical basis for further research on the correlation of protein oxidation in meat and meat products.

Author contributions
Sha Qu mainly writes manuscripts Dong Sun and Ting Hu are responsible for collating the data Gang Hao are instruments support.

Funding
This research is supported by "the Fundamental Research Funds for the Central Universities", Southwest Minzu University (2021XJTD02).

Data availability
Data is provided within the manuscript or supplementary information files.

Declarations

Ethical approval
Ethics approval was not required for this research.

Consent for publication
Not applicable.

Competing interests
The authors declare no competing interests.

Received: 8 February 2024 / Accepted: 25 February 2025
Published online: 22 April 2025

References

1. Li X, Li Y, Hua Y, Qiu A, Yang C, Cui S. Effect of concentration, ionic strength and freeze-drying on the heat-induced aggregation of soy proteins. Food Chem. 2007;104(4):1410–7. https://doi.org/10.1016/j.foodchem.2007.02.003.
2. Wang WQ, Sheng HB, Zhou JY, Yuan PP, Zhang XF, Lu ML, et al. The effect of a variable initial pH on the structure and rheological properties of Whey protein and monosaccharide gelation via the Maillard reaction. Int Dairy J. 2021;113:104896. https://doi.org/10.1016/j.idairyj.2020.104896.
3. Wang N, Hu L, Guo X, Zhao Y, Deng X, Lei Y, et al. Effects of malondialdehyde on the protein oxidation and protein degradation of Coregonus Peled myofibrillar protein. J Food Meas Charact. 2022;16(5):3459–68. https://doi.org/10.1007/S11694-022-01452-9.
4. Wei X, Pan T, Liu H, Boga LAI, Hussian Z, Suleman R, et al. The effect of age on the myosin thermal stability and gel quality of Beijing Duck breast. Food Sci Anim Resour. 2020;40(4):588–600. https://doi.org/10.5851/kosfa.2020.e36.
5. Du X, Zhao M, Pan N, Wang S, Xia X, Zhang D. Tracking aggregation behaviour and gel properties induced by structural alterations in myofibrillar protein in mirror carp (Cyprinus carpio) under the synergistic effects of pH and heating. Food Chem. 2021;362:130222. https://doi.org/10.1016/j.foodchem.2021.130222.
6. Zhang B, Fang CD, Hao GJ, Zhang YY. Effect of kappa-carrageenan oligosaccharides on myofibrillar protein oxidation in peeled shrimp (Litopenaeus vannamei) during long-term frozen storage. Food Chem. 2018;245:254–61. https://doi.org/10.1016/j.foodchem.2017.10.112.
7. Liu J, Yu Z, Yang L, Zhang M, Li C, Shao J. Effects of tetrasodium pyrophosphate coupled with soy protein isolate on the emulsion gel properties of oxidative myofibrillar protein. Food Chem. 2023;408:135208. https://doi.org/10.1016/j.foodchem.2022.135208.
8. Señorans FJ, Ibáñez E, Cifuentes A. New trends in food processing. Crit Rev Food Sci Nutr. 2003;43(5):507–26. https://doi.org/10.1080/10408690390246341.
9. Cao Y, True AD, Chen J, Xong Y. Dual role (anti- and pro-oxidant) of Gallic acid in mediating myofibrillar protein gelation and gel in vitro digestion. J Agric Food Chem. 2016;64:3054–61. https://doi.org/10.1021/acs.jafc.6b00314.
10. Xin KQ, Tian K, Yu QL, Han L. High oxygen-modified packaging (HiOx-MAP) mediates HIF-1α regulation of tenderness changes during postmortem aging of Yak meat. Food Chem. 2023;17:100573. https://doi.org/10.1016/j.fochx.2023.100573.
11. Zhang X, Zhu L, Song L, Song L, Shi S, Liu H, et al. Combined treatment of lactic acid-ultrasound-papain on Yak meat and its tenderization mechanism. Meat Sci. 2023;196:109043. https://doi.org/10.1016/j.meatsci.2022.109043.
12. Zheng S, Chen X, Wang J, Guo T, Liu L, Chen J, et al. Effect of pH on gelling properties of myofibrillar protein in large yellow croaker (Pseudosciaena croeca). J Biobased Mater Bioenergy. 2019;13(2):264–8. https://doi.org/10.1166/jbmb.2019.1837.
13. Xiong L, Blanchard SP, Ooizumi T, Ma Y. Hydroxyl radical and Ferryl-Generating systems promote gel network formation of myofibrillar protein. J Food Sci. 2010;75(2):C215–21. https://doi.org/10.1111/j.1750-3841.2009.01511.x.
14. Jia G, Nirasawa S, Ji X, Luo Y, Liu H. Physicochemical changes in myofibrillar proteins extracted from pork tenderloin thawed by a high-voltage electrostatic field. Food Chem. 2018;240:910–6. https://doi.org/10.1016/j.foodchem.2017.07.13.
15. Jian H, Xiong Y, Guo F, Huang X, Adhikari B, Chen J. Gelation enhancement of soy protein isolate by sequential low- and ultrahigh-temperature two-stage preheating treatments. Int J Food Sci Technol. 2014;49(12):2529–37. https://doi.org/10.1111/ijfs.12694.
16. Jiang W, He Y, Xiong S, Liu Y, Yin T, Hu Y, et al. Effect of mild Ozone oxidation on structural changes of silver carp (Hypophthalmichthys molitrix) myosin. Food Bioprocess Technol. 2017;10(2):370–8. https://doi.org/10.1007/s11947-016-1828-5.
17. Kang D, Zou Y, Cheng Y, Xing L, Zhou G, Zhang W. Effects of power ultrasound on oxidation and structure of beef proteins during curing processing. Ultrason Sonochem. 2016;33:47–53. https://doi.org/10.1016/j.ultsonch.2016.04.024.
18. Kong XZ, Li XH, Wang HJ, Hua YF. Effect of lipoxygenase activity in defatted soybean flour on the gelling properties of soybean protein isolate. Food Chem. 2008;106(3):1093–99. https://doi.org/10.1016/j.foodchem.2007.07.050
19. Delles RM, Xiong YL. The effect of protein oxidation on hydration and water-binding in pork packaged in an oxygen-enriched atmosphere. Meat Sci. 2014;97(2):181–8. https://doi.org/10.1016/j.meatsci.2014.01.022.
20. Han M, Zhang Y, Fei Y, Xu X, Zhou G. Effect of microbial transglutaminase on NMR relaxometry and microstructure of pork myofibrillar protein gel. Eur Food Res Technol. 2009;228:665–70. https://doi.org/10.1007/s00217-008-0976-x.
21. Ni N, Wang Z, Hang Z, Pan H, Mu G, Zhang D. Effect of pH on Heat-Induced gel of myofibrillar protein from lamb M. longissimus dorsi muscle. Scientia Agricultura Sinica. 2013;46(17):3680–7. https://doi.org/10.3864/j.issn.0578-1752.2013.17.017.
22. Boronat S, García-Santamarina S, Hidalgo E. Gel-free proteomic methodologies to study reversible cysteine oxidation and irreversible protein carbonyl formation. Free Radic Res. 2015;49(4):494–510. https://doi.org/10.3109/10715762.2015.1009053.
23. Irwin JA, Østdal H, Davies MJ. Myoglobin-Induced oxidative damage: evidence for radical transfer from oxidized myoglobin to other proteins and antioxidants. Arch Biochem Biophys. 1999;362(1):94–104. https://doi.org/10.1006/abbi.1998.0987.
24. Chan JT, Omana DA, Betti M. Effect of ultimate pH and freezing on the biochemical properties of proteins in Turkey breast meat. Food Chem. 2021;127(1):109–17. https://doi.org/10.1016/j.foodchem.2010.12.095.
25. Zhang Z, Xiong Z, Lu S, Walayat N, Hu C, Xiong H. Effects of oxidative modification on the functional, conformational and gelling properties of myofibrillar proteins from Culter alburnus. Int J Biol Macromol. 2020;162:1442–52. https://doi.org/10.1016/j.ijbiomac.2020.08.052.
26. Li X, Liu C, Wang J, Zhou K, Yi S, Zhu W, et al. Effect of hydroxyl radicals on biochemical and functional characteristics of myofibrillar protein from large yellow croaker (Pseudosciaena crocea). J Food Biochem. 2020;44(1):e13084. https://doi.org/10.1111/jfbc.13084.
27. Shen H, Zhao M, Sun W. Effect of pH on the interaction of Porcine myofibrillar proteins with pyrazine compounds. Food Chem. 2019;287:93–9. https://doi.org/10.1016/j.foodchem.2019.02.060.

28. Ma Y, Xiong S, You J, Yang H, Hu Q, Yin T. Effects of vacuum chopping on physicochemical and gelation properties of myofibrillar proteins from silver carp (Hypophthalmichthys molitrix). Food Chem. 2018;245:557–63. https://doi.org/10.1016/j.foodchem.2017.10.139.
29. Wu W, Wu X, Hu Y. Structural modification of soy protein by the lipid peroxidation product acrolein. LWT - Food Sci Technol. 2010;43(1):133–40. https://doi.org/10.1016/j.lwt.2009.05.006.
30. Estévez M, Kylli P, Puolanne E, Kivikari R, Heinonen M. Fluorescence spectroscopy as a novel approach for the assessment of myofibrillar protein oxidation in oil-in-water emulsions. Meat Sci. 2008;80(4):1290–6. https://doi.org/10.1016/j.meatsci.2008.06.004.
31. Wang Z, He Z, Gan X, Li H. Effect of Peroxyl radicals on the structure and gel properties of isolated rabbit meat myofibrillar proteins. Int J Food Sci Technol. 2018;53(12):2687–96. https://doi.org/10.1111/ijfs.13878.
32. Wu W, Zhang C, Kong X, Hua Y. Oxidative modification of soy protein by Peroxyl radicals. Food Chem. 2009;116(1):295–301. https://doi.org/10.1016/j.foodchem.2009.02.049.
33. Yan S, Xu J, Zhang X, Xie F, Zhang S, Jiang L, et al. Effect of pH-shifting treatment on the structural and functional properties of soybean protein isolate and its interactions with (-)-epigallocatechin-3-gallate. Process Biochem. 2021;101:190–8. https://doi.org/10.1016/j.procbio.2020.10.016.
34. Lu H, Zhang L, Li Q, Luo Y. Comparison of gel properties and biochemical characteristics of myofibrillar protein from Bighead carp (Aristichthys nobilis) affected by frozen storage and a hydroxyl radical-generation oxidizing system. Food Chem. 2017;223:96–103. https://doi.org/10.1016/j.foodchem.2016.11.143.
35. Stadtman ER, Levine RL. Free radical-mediated oxidation of free amino acids and amino acid residues in proteins. Amino Acids. 2003;25(3–4):207–18. https://doi.org/10.1007/s00726-003-0011-2.
36. Zhu W, Huan H, Bu Y, Li X, Shiuan D, Li J, et al. Effects of hydroxyl radical induced oxidation on water holding capacity and protein structure of Jumbo squid (Dosidicus gigas) mantle. Int J Food Sci Technol. 2019;54(6):2159–68. https://doi.org/10.1111/ijfs.14123.
37. Souissi N, Jridi M, Nasri R, Slama RB, Njeh M, Nasri M. Effects of the edible cuttlefish gelatin on textural, sensorial and physicochemical quality of octopus sausage. LWT - Food Sci Technol. 2016;65:18–24. https://doi.org/10.1016/j.lwt.2015.07.051.
38. Wu W, Zhang C, Hua Y. Structural modification of soy protein by the lipid peroxidation product malondialdehyde. J Sci Food Agric. 2009;89(8):1416–23. https://doi.org/10.1002/jsfa.3606.
39. Shimada K, Cheftel JC. Sulfhydryl group/disulfide bond interchange reactions during heat-induced gelation of Whey protein isolate. J Agricultural Food Chem. 1989;37:161–8. https://doi.org/10.1021/jf00085a038.
40. Xia M, Chen Y, Guo J, Feng X, Yin X, Wang L, et al. Effects of oxidative modification on textural properties and gel structure of pork myofibrillar proteins. Food Res Int. 2019;121:678–83. https://doi.org/10.1016/j.foodres.2018.12.037.
41. Zhang Z, Regenstein JM, Zhou P, Yang Y. Effects of high intensity ultrasound modification on physicochemical property and water in myofibrillar protein gel. Ultrason - Sonochemistry. 2017;34(e 960–967). https://doi.org/10.1016/j.ultsonch.2016.08.008.
42. Wang J, Yang Y, Kang D, Tang X, Zhang X, Ni W. Effects of ultrasound on chemical forces and water holding capacity study of Heat-Induced myofibrillar protein gel. Scientia Agricultura Sinica. 2017;50(12):2349–58. https://doi.org/10.3864/j.issn.0578-1752.2017.12.015.

Publisher's note